Action-at-a-distance mutations induced by 8-oxo-7,8-dihydroguanine are dependent on APOBEC3

Ruriko Fukushima[#], Tetsuya Suzuki[#], Akari Kobayakawa, Hiroyuki Kamiya[*]

Graduate School of Biomedical and Health Sciences, Hiroshima University, 1-2-3 Kasumi, Minami-ku, Hiroshima 734-8553, Japan

[#]Equal contributions.

Running Head: Mutation by oxidised guanine and APOBEC3

*Corresponding author. Graduate School of Biomedical and Health Sciences, Hiroshima University, 1-2-3 Kasumi, Minami-ku, Hiroshima 734-8553, Japan. Email: hirokam@hiroshima-u.ac.jp.

Abstract

DNA oxidation is a serious threat to genome integrity and involved in mutations and cancer initiation. The G base is most frequently damaged, and 8-oxo-7,8-dihydroguanine (G^O, 8-hydroxyguanine) is one of the predominant damaged bases. In human cells, G^O causes a G:C→T:A transversion mutation at the modified site, and also induces untargeted substitution mutations at the G bases of 5'-GpA-3' dinucleotides (action-at-a-distance mutations). The 5'-GpA-3' sequences are complementary to the 5'-TpC-3' sequences, the preferred substrates for apolipoprotein B mRNA-editing enzyme, catalytic polypeptide-like 3 (APOBEC3) cytosine deaminases, and thus their contribution to mutagenesis has been considered. In this study, APOBEC3B, the most abundant APOBEC3 protein in human U2OS cells, was knocked down in human U2OS cells, and a G^O-shuttle plasmid was then transfected into the cells. The action-at-a-distance mutations were reduced to ~25% by the knockdown, indicating that G^O-induced action-at-a-distance mutations are highly dependent on APOBEC3B in this cell line.

Keywords:

8-oxo-7,8-dihydroguanine;

8-hydroxyguanine;

action-at-a-distance mutation;

APOBEC3;

cytosine deaminase

Introduction

Reactive oxygen species (ROS) constitute a dangerous menace to genome integrity and produce various types of DNA damage, including base modifications, base loss, and strand breaks. The DNA damages induce mutations, and in the worst case, cancer [1–3]. They are also related to cell death, neurodegeneration, and aging. The G base is most vulnerable to attacks by ROS, due to its lowest oxidation potentials [4,5]. 8-Oxo-7,8-dihydroguanine (G^O, also known as 8-hydroxyguanine) is one of the major damaged G bases [6–8], and causes G:C→T:A and A:T→C:G transversions when formed by the oxidations of DNA and dGTP, respectively, in mammalian cells [9–17].

In addition to the G:C→T:A mutations at the damaged sites, G^O causes untargeted base substitutions in human cells [18–20]. In particular, the substitutions at the G bases of 5'-GpA-3' dinucleotides (the C bases of 5'-TpC-3') are most frequent and all types of base substitutions are found at these G:C base pairs. These action-at-a-distance mutations are promoted by the knockdown of Werner syndrome protein, although the reasons for this effect remain unknown [18,19]. Interestingly, OGG1, the major DNA glycosylase involved in the base excision repair (BER) of G^O, seems to be associated with the mutations since they are decreased by the OGG1 knockdown [21]. The damaged base removal by this BER protein may trigger the untargeted mutations, and this phenomenon was named the 'OGG1 paradox.'

The C bases of 5'-TpC-3' dinucleotides are the preferred sequence for APOBEC3, apolipoprotein B mRNA-editing enzyme, catalytic polypeptide-like 3 (APOBEC3) cytosine deaminases except for APOBEC3G, which targets 5'-CpC-3' [22]. As described above, the G^O-

induced untargeted mutations are formed at the G/C bases of 5'-GpA-3'/5'-TpC-3' sequences and the G/C bases are mutated at multiple positions in identical DNA molecules. These cluster mutations are features shared with the action-at-a-distance and APOBEC3-mediated mutations. A recent analysis of cancer cells by next-generation sequencing revealed that various types of cancers possess APOBEC-associated mutations (single-base substitution (SBS) signatures 2 and 13) [23]. The G:C→T:A transversions, the same type of mutation induced at G^O sites, are also important mutations found in cancer cells and attributed to ROS (SBS18) [23]. The action-at-a-distance mutations may be linked to ROS/G^O and APOBEC, which are important factors for mutation induction in cancer cells.

Thus, the involvement of APOBEC3 enzymes in the induction of the action-at-a-distance mutations must be elucidated to understand the mutagenesis mechanisms. We focused on APOBEC3B, since this molecule is localized in the nucleus [22,24] and expressed in human U2OS cells [25]. Additionally, our reverse transcription-quantitative PCR (RT-qPCR) analysis confirmed that APOBEC3B is the major APOBEC molecule in this cell line (see 'Results' section). We knocked down APOBEC3B in U2OS cells and examined the mutations produced when a G^O-containing replicative plasmid DNA was introduced into the knockdown cells. The base substitutions at the G bases of 5'-GpA-3' dinucleotides were reduced by ~75% in the knockdown cells, indicating that APOBEC3 is primarily responsible for the action-at-a-distance mutations.

Materials and Methods

Materials

5'-Phosphorylated oligodeoxyribonucleotides (ODNs) containing G or G^O for plasmid construction were synthesized and purified by HPLC, as described previously (Supplementary Table S1) [26–28]. ODNs used for RT-qPCR were purchased from Integrated DNA Technologies (Coralville, IA, USA) and Hokkaido System Science (Sapporo, Japan). The DsiRNA against APOBEC3B (si-APOBEC3B-A) and the nontargeting DsiRNA (DS NC1, control RNA) were purchased from Integrated DNA Technologies. The Stealth RNAi siRNA against APOBEC3B (si-APOBEC3B-B) and the Stealth RNAi Negative Control Medium GC duplex (%GC 48) were purchased from Thermo Fisher Scientific (Waltham, MA, USA). Phusion DNA polymerase, *Taq* DNA ligase, Dam DNA methyltransferase, T5 exonuclease, Fpg, Nb.*Bbv*C I, Nt.*Bbv*C I, and *Dpn* I were from New England Biolabs (Ipswich, MA, USA). *Xba* I was from Takara (Kusatsu, Japan).

Cell line and cell culture

The human osteosarcoma U2OS cells were obtained from American Type Culture Collection (Manassas, VA, USA, ATCC HTB-96). U2OS cells were cultured in Dulbecco's modified Eagle's medium (Nissui Pharmaceutical, Tokyo, Japan) containing 10% (v/v) fetal bovine serum and 1× Antibiotic-Antimycotic Mixed Stock Solution (Nacalai Tesque, Kyoto, Japan) at 37°C in a humidified atmosphere with 5% CO_2.

Plasmid DNA construction

The double-stranded pSB189KL-BC12(D12) plasmid DNAs containing G or G^O were constructed from the single-stranded (ss) form of pSB189KL-BC(D12) and the 5'-phosphorylated G or G^O ODN (Supplementary Fig. S1, Supplementary Table S1), as described previously [20,29]. Namely, the ODN hybridized to ss DNA was extended by Phusion DNA polymerase and the extended 3'-end and the phosphorylated 5'-end were joined by *Taq* DNA ligase. These polymerase and ligase reactions were simultaneously conducted at 65°C. The double-stranded plasmid DNA was then treated with Dam DNA methyltransferase and T5 exonuclease at 37°C to give the bacterial methylation pattern and to digest nicked/linear DNAs, respectively. The DNA was purified with a PureLink PCR Purification Kit (Thermo Fisher Scientific) and ethanol precipitation.

Fpg treatment

The G- and G^O-plasmid DNAs (200 ng) were treated with Fpg (0.4 units), *Xba* I (7.5 units), and Nb.*Bbv*C I or Nt.*Bbv*C I (5 units) at 37°C for 1 h. After enzyme inactivation at 80°C for 20 min and ethanol precipitation, the DNA was dissolved in 5 μL of H_2O, mixed with 15 μL of formamide, heated at 70°C for 5 min, and run on a 1% agarose gel. The gel was stained with GelRed (Biotium, Fremont, CA, USA).

siRNA and plasmid DNA introductions and *supF* mutation analyses

Introductions of siRNA and plasmid DNA into U2OS cells were performed as described previously, with slight modifications [21]. Briefly, U2OS cells (1.0×10^5 cells/well in 12-well

plates) were reverse transfected with 0.25 μL Lipofectamine RNAiMAX (Thermo Fisher Scientific) and 2.5 nM siRNA. The DS NC1 RNA or the Stealth RNAi Negative Control Medium GC duplex was used as the negative control RNA. At 24 h after siRNA introduction, 200 ng of the plasmid DNA (59 fmol) was introduced with Lipofectamine 2000 (Thermo Fisher Scientific). After 48 h, the plasmid DNA was extracted from the cells and unreplicated plasmid was digested with *Dpn* I, as described previously [19]. The replicated plasmid was introduced into the indicator *Escherichia coli* RF01 strain to calculate the *supF* mutant frequency [30]. The mutation spectra of the *supF* gene were analyzed by sequencing the plasmids obtained from the colonies on the selection plates.

RT-qPCR

Total RNA was extracted with ISOGEN II (Nippon Gene, Tokyo, Japan) at 24, 48, and 72 h after siRNA introduction, and then reverse-transcribed to cDNA with a High-Capacity RNA-to-cDNA kit (Thermo Fisher Scientific) according to the manufacturer's protocol. qPCR was performed using TB Green *Premix Ex Taq* II (Tli RNase H Plus) (Takara) and Thermal Cycler Dice Real Time System Single (Takara) with a standard protocol. The respective mRNA levels of APOBEC3s were calculated relative to the GAPDH mRNA level as 1.0. Primers for RT-qPCR are listed in Supplementary Table S1.

Western blotting

At 24, 48, and 72 h after siRNA introduction, cells were lysed by radioimmunoprecipitation (RIPA) buffer to obtain whole cell extracts. The extracts were fractionated by 12% SDS-polyacrylamide gel electrophoresis, and proteins were transferred to PVDF membranes. The membranes were then blocked with 5% skimmed milk in phosphate-buffered saline containing 0.05% Tween 20 (PBS-T) for 1 h at room temperature. Rabbit anti-APOBEC3B (Abcam plc, Cambridge, UK, catalogue No. ab184990) and mouse anti-β-tubulin (Wako, Osaka, Japan, catalogue No. 014-25041) antibodies, and anti-rabbit and anti-mouse IgGs conjugated with horseradish peroxidase (GE Healthcare, Piscataway, NJ, USA) were used as primary and secondary antibodies, respectively. The proteins were detected using ImmunoStar LD (Wako) for APOBEC3B and EzWestLumi Plus (ATTO, Tokyo, Japan) for β-tubulin, scanned with an ImageQuant LAS 4000 mini image analyzer (GE Healthcare), and quantified with the ImageJ software [31].

Statistics

Statistical comparisons were performed between the control and APOBEC3B-knockdown cells using the Student's *t*-test. A *P* value less than 0.05 was considered statistically significant.

Results

APOBEC3B knockdown

Seven human APOBEC3 proteins have been identified (APOBEC3A, APOBEC3B, APOBEC3C, APOBEC3DE (APOBEC3D), APOBEC3F, APOBEC3G, and APOBEC3H) [22]. First, we examined the APOBEC3 expression patterns in human U2OS cells under our experimental conditions. The RT-qPCR analysis revealed that the amounts of mRNAs were in the order of APOBEC3B > APOBEC3C > APOBEC3F > the others (Supplementary Fig. S2, open columns). Thus, APOBEC3B is the major APOBEC deaminase at the RNA level in U2OS cells, and we focused on this molecule as the knockdown target. APOBEC3B has the nuclear localizing signal (NLS) at its N-terminus and is constitutively localized in the nucleus [24]. This subcellular localization property also rationalized the choice of APOBEC3B as the objective. APOBEC3A, the other important molecule for tumorigenesis [22], was scarcely expressed in U2OS cells.

We designed an effective and specific siRNA against APOBEC3B (si-APOBEC3B-A, Supplementary Table S1 and Supplementary Fig. S3). The introduction of the designed siRNA reduced both the APOBEC3B mRNA and protein (Fig. 1), with efficiencies of 92% and 74% at the mRNA and protein levels respectively, after 24 h. Moreover, we examined APOBEC3 mRNAs by RT-qPCR analyses and confirmed that the RNA interference was specific for APOBEC3B: the siRNA treatment virtually had no impact on the amounts of other APOBEC3 mRNAs (Supplementary Fig. S2, closed columns). Note that the APOBEC3A mRNA was undetected in two of the three experiments.

Reduced mutant frequency by APOBEC3B knockdown

We placed the G^O base in the region outside the *supF* gene, as described previously [19,20]. The G^O was located 14-bases downstream of the 3'-terminus of the gene, at "position 176". Basically, the G→T mutation at the G^O site does not produce *supF* mutants, and this enables preferential detection of the action-at-a-distance mutations. In addition, a 12-bp random sequence (barcode) was placed downstream of the gene to distinguish whether multiple *supF* mutant plasmid DNAs with the same mutation(s) are derived from different original DNA or amplified in U2OS and/or *E. coli* cells from a single DNA molecule, and to reduce the bias in the mutation spectrum by excluding the amplified DNA (Supplementary Fig. S1) [33,34]. The G- and G^O-plasmid DNAs were prepared by ODN hybridization to ss DNA, DNA polymerase plus ligase reactions, and adenine methylation (Supplementary Fig. S4). The presence of G^O was confirmed by Fpg treatment of the G^O-plasmid (Supplementary Fig. S5). The two plasmid DNAs were transfected into U2OS cells treated with the siRNA against APOBEC3B. We used plasmid DNAs obtained in three independent plasmid construction experiments for the three transfection experiments. After isolation, the replicated plasmid was introduced into *E. coli* RF01 cells to select *supF* mutants [30].

The presence of the oxidized G base increased the total *supF* mutant frequency in the control cells (Fig. 2). The siRNA treatment had little impact, if any, on the *supF* mutant frequency for the control plasmid DNA (176G). In contrast, the APOBEC3B knockdown significantly reduced the mutant frequency induced by G^O as expected (Fig. 2), suggesting the involvement of this deaminase in the action-at-a-distance mutations. The mutant frequency in the knockdown cells was ~half of that in the control cells.

The presence of G^O and the APOBEC3B knockdown did not affect the total numbers of bacterial colonies on titer plates, indicating little, if any, impact on replication efficiency in U2OS cells (data not shown).

Reduced action-at-a-distance mutations by APOBEC3B knockdown

We then analyzed the mutations in the *supF* gene in detail (Supplementary Tables S2 and S3, Tables 1-3). The knockdown apparently reduced base substitution mutations, especially at G:C pairs (Table 1). Note that the percentages in this table were calculated based on the numbers of total colonies analyzed since multiple mutations were frequently found in identical DNA molecules. As described above, APOBEC3B deaminates the C bases of 5'-TpC-3' dinucleotides. The knockdown decreased the proportion of base substitutions at the G bases of 5'-GpA-3' sequences in the strand corresponding to the sense strand of the *supF* gene (Table 3). No colonies that have both the substitutions at the G bases of 5'-GpA-3' and the targeted mutation at the G^O site were found (Supplementary Tables S2 and S3).

We finally calculated the F_{GpA} value, the G→X (X = A, C, and T) mutation frequencies at 5'-GpA-3', based on the total *supF* mutant frequencies, the base substitution ratios, and the numbers of substitutions at 5'-GpA-3' per plasmid DNA molecule containing substitution(s) (Fig. 3) [19]. The decrease in the F_{GpA} value by the APOBEC3B knockdown was more evident than that in the mutant frequency. The F_{GpA} value for the G^O-plasmid DNA in the knockdown cells was 1.2×10^{-3}, a quarter of that in the control cells (4.8×10^{-3}). Interestingly, the APOBEC3B knockdown also reduced the value for the control plasmid DNA. Thus, the knockdown lowered the base

substitutions at 5'-GpA-3' for the modified and unmodified plasmid DNAs. However, the F_{GpA} values were decreased by 0.4×10^{-3} and 3.6×10^{-3} for the G- and G^O-plasmid groups, respectively, indicating that the effect of knockdown was much larger for the G^O-plasmid than the G-plasmid (Fig. 3). These results indicated that APOBEC3B is the major deaminase responsible for the action-at-a-distance mutations induced by the G^O base in U2OS cells.

This conclusion was supported by the knockdown experiment using another siRNA against APOBEC3B (si-APOBEC3B-B, Supplementary Table S1, Supplementary Figs. S3 and S6-S8). The knockdown efficiencies were 91% and 57% at the mRNA and protein levels, respectively, at 24 h after siRNA introduction. The knockdown using this siRNA reduced the *supF* mutant frequency and the F_{GpA} value, in line with the results shown in Figs. 2 and 3. Thus, the results obtained with the different siRNAs support the same conclusion.

Discussion

The major objective of this study was to examine whether APOBEC3 induces the action-at-a-distance mutations. The involvement of APOBEC3 was expected since (i) the mutations were observed at the G bases of 5'-GpA-3' sequences that are complementary to the C bases of 5'-TpC-3' sequences, the preferential substrate for most APOBEC3 enzymes, (ii) the mutations were found as clusters, and (iii) the untargeted mutations induced by U:G/T:G mismatches were reportedly decreased by the APOBEC3 knockdown [35]. We surmised that APOBEC3B would contribute to the mutations, due to its abundance in U2OS cells and its nuclear localization. Indeed, the F_{GpA}

value, the substitution mutation frequencies at the G bases of 5'-GpA-3', was reduced by ~75% upon the knockdown of APOBEC3B (Fig. 3). Thus, among the various cytosine deaminases, APOBEC3B has the largest contribution to the action-at-a-distance mutations induced by the G^O base in U2OS cells.

We counted the numbers of colonies carrying a single 5'-GpA-3' substitution and those carrying multiple 5'-GpA-3' substitutions for the control and knockdown cells, based on the data shown in Supplementary Tables S2 and S3. Among the 68 analyzed colonies, 30 and 17 had single and multiple substitutions, respectively, for the control cells. In contrast, for the knockdown cells, 26 and 6 among the 68 analyzed colonies carried single and multiple substitutions, respectively. Thus, the ratio of colonies carrying a single 5'-GpA-3' substitution to those carrying multiple 5'-GpA-3' substitutions were increased by the APOBEC3B knockdown, in addition to the decreased mutant frequency (Supplementary Fig. S9). These numbers were calculated without considering the barcode overlap, but quite similar results were also obtained when the barcode-overlapped data were excluded. Thus, the APOBEC3B knockdown decreased clustered 5'-GpA-3' substitutions. The deaminase reportedly moves 3-dimensionally and thus efficiently deaminates multiple targets [36]. The disappearance of multiple 5'-GpA-3' substitutions by the APOBEC3B knockdown agreed with the enzyme's ability to induce cluster mutations.

The untargeted mutations at the 5'-GpA-3' sites were not distributed equally in the *supF* gene, and positions 5, 91, and 126 were hotspots (Supplementary Table S3). The flanking sequences of positions 5, 91, and 126 are 5'-TTGAT-3' (5'-ATCAA-3'), 5'-CAGAC-3' (5'-GTCTG-3'), and 5'-TCGAA-3' (5'-TTCGA-3'), respectively. Meanwhile, the sequence preference

of APOBEC3B is reportedly 5'-TCA-3' and the protein favors 5'-RTCA-3' over 5'-YTCA-3' (R = A/G and Y = C/T) [37,38]. The sequence around position 5 matches RTCA, whereas those around positions 91 and 126 are 5'-RTCT-3' and 5'-YTCG-3', respectively. In addition, the *supF* gene encodes a (pre-)tRNA molecule and thus might form a stem-loop structure. The possible secondary structures of the gene (from positions –30 to 192, lower (antisense) strand) were examined by "DNA Folding Form" in the mFold web server (http://www.unafold.org/mfold/applications/dna-folding-form.php) [39]. Position 5 is located on a loop in the predicted secondary structure with the lowest Δ*G* value, but positions 91 and 126 are within a stem (Supplementary Fig. S10). The APOBEC3B knockdown seemed to reduce mutations at these positions, suggesting that the mutations at positions 91 and 126 also originated from the cytosine deamination by this enzyme. However, we should consider the presence of silent mutations in the *supF* gene that do not confer antibiotic resistance to the indicator bacterial strain. The next generation sequencing method could resolve this issue and other mutational hotspots might be found [40]. Further studies would provide pivotal information on hotspot sequences.

The APOBEC3B knockdown reduced the F_{GpA} values for both the unmodified plasmid and the G^{O}-modified plasmid (Fig. 3). Thus, the C deamination contributed to the background *supF* mutation, at least under our experimental conditions. APOBEC3B preferentially catalyzes the deamination reaction of C bases in ss DNA [22]. During replication, the template strands before nucleotide incorporation are in the ss state, and "naked" C bases in this situation could be substrates for the enzyme. The pSB189KL-BC12(D12) plasmid used in this study contains the SV40 origin of replication in the upstream region near the *supF* gene (Supplementary Fig. 1) [20]. Thus, the

lower (antisense) strand of the *supF* gene would be the leading strand template. In general, a lagging strand template (the upper strand of the gene) is considered to be a preferential substrate for APOBEC3B as compared to a leading strand template. Thus, C bases of 5'-TpC-3' dinucleotides on the upper strand of the *supF* gene were possibly deaminated by APOBEC3B. However, the effects of the APOBEC3B knockdown on the base substitution mutation frequency at C bases of 5'-TpC-3' sequences were unclear, in contrast to the F_{GpA} value, since this type of mutations occurred with low and quite-variable frequencies (Supplementary Table S4). Therefore, the deamination reactions during DNA replication do not clearly explain the biased background mutations and APOBEC3B knockdown effects. As we described previously, the strand corresponding to the *supF* upper strand was synthesized *in vitro* [20]. This might be associated with the background mutations, although further experiments are needed for clarification.

Chen *et al*. used HeLa cells that express APOBEC3B, APOBEC3C, and APOBEC3F in their U:G/T:G mismatch-induced untargeted mutation experiments [35]. Although single knockdowns of these APOBEC3s did not result in drastic reductions of the mutation frequencies, the APOBEC3B knockdown altered the mutation sites most effectively. The authors concluded that APOBEC3B was the most important contributor to mutations, in line with our findings. The results obtained in the two laboratories should be carefully compared, since different cell lines, plasmid DNAs, and transfection methods were employed. However, the common conclusion that APOBEC3B (APOBEC3, in general) was the protein responsible for the untargeted mutations is important, since it indicates the involvement of the deaminase in the mutagenic pathways originating from mismatches and an oxidatively damaged base.

Recent analysis suggested that APOBEC3A rather than APOBEC3B are associated with genome mutations in many cancer cells [41–43]. Thus, we do not intend to conclude that only APOBEC3B induces the action-at-a-distance mutations. APOBEC3A is a myeloid lineage-specific cytosine deaminase and APOBEC3A expression was undetectable in many cultured cell lines [35,44]. Moreover, the expression of exogenous APOBEC3A decreases cell viability [45]. Thus, further studies are pivotal to examine untargeted mutations using cells with detectable but nontoxic amounts of APOBEC3A. However, the most important point is that this study clearly indicated that at least one of the APOBEC3 proteins is involved in the untargeted mutations that originate from G^O. Taken together with the results of Chen *et al*. [35], a single or multiple APOBEC3 enzymes would be associated with the untargeted mutations although the majorly responsible APOBEC member(s) are dependent on cell type.

Targeted mutations at the G^O site were absent in all colonies containing the substitutions at the G bases of 5'-GpA-3' in this study (Supplementary Tables S2 and S3) and previous studies [18-21]. This supports the hypothesis that the G^O removal by OGG1 triggers the untargeted mutations. As discussed in previous papers, according to the report by Chen *et al*. [35], DNA containing an abasic site is possibly nicked by AP endonuclease, incorrectly occupied by mismatch repair proteins, and deaminated by APOBEC3 protein(s). This proposed mechanism is tested in our laboratory.

The *supF* gene is placed between the SV40 and pBR327 origins essential for replication in human and bacterial cells, respectively (Supplementary Fig. 1), and the positions –88 and 242 are their closest ends. Thus, untargeted mutations are basically detectable from position –87 to position

241 when we assume that any substitution mutations within the origin regions do not allow the plasmid replication. These positions are 262- and 66-bp, respectively, distant from the G^O position. Plasmid DNA with longer 'linker' regions may be used to know mutations at more distant positions. However, we use the plasmid DNA with short linkers to reduce large deletion mutants that lead to increasing complexity of mutant analysis. Position –280, albeit in the SV40 origin region, was the farthest site where untargeted mutation at 5'-GpA-3' was observed [20].

One may think that the introduction of G^O-plasmid promoted APOBEC3B expression resulting in the observed untargeted mutations. However, neither the G^O- nor the G-plasmid affected the amount of APOBEC3B at 8, 24, and 48 h after transfection (Supplementary Fig. S11). Thus, G^O induced the action-at-a-distance mutations independently of APOBEC3B upregulation, but dependently on OGG1 [21], at least under our experimental conditions.

The *supF* mutant frequencies of the G- and G^O-plasmid DNAs were 2.5 (± 0.1) × 10^{-4} and 2.4 (± 0.3) × 10^{-4}, respectively (the means ± standard errors, n=3), when they were directly introduced into the indicator bacterial cells. Thus, most of the mutations, at least observed in the G^O experimental groups, were generated in the transfected U2OS cells.

In conclusion, the APOBEC3B knockdown strongly suppressed the action-at-a-distance mutations, the base substitutions at the 5'-GpA-3' sites, in U2OS cells. Therefore, we found clear evidence that the cytosine deaminases APOBEC3's are pivotal players that participate in the untargeted mutagenic process originated from by the G^O base. ROS/G^O and APOBEC3 are presumed to cause some mutagenic events found in cancer cells, and the results obtained in this study provide a possible link between these two important factors [23].

Acknowledgements

This work was supported in part by the Japan Society for the Promotion of Science (JSPS) KAKENHI (grant numbers JP 19H04278 and JP 22H03751 to H.K., and JP 20K12181 to T.S.) and Japan Science and Technology Agency (JST) SPRING (grant number JPMJSP2132 to R.F.).

Conflict of interest statement: None declared.

Data availability

The datasets generated for this study are available on request to the corresponding author.

References

1. Halliwell, B. and Aruoma, O. I. (1991) DNA damage by oxygen-derived species. Its mechanism and measurement in mammalian systems. FEBS Lett., 281, 9–19.
2. Ames, B. N., Shigenaga, M. K. and Hagen, T. M. (1993) Oxidants, antioxidants, and the degenerative diseases of aging. *Proc. Natl. Acad. Sci. USA*, 90, 7915–7922.
3. Jackson, A. L. and Loeb, L. A. (2001) The contribution of endogenous sources of DNA damage to the multiple mutations in cancer. *Mutat. Res.*, 477, 7–21.
4. Seidel, C. A. M., Schulz, A. and Sauer, M. H. M. (1996) Nucleobase-specific quenching of fluorescent dyes. 1. Nucleobase one-electron redox potentials and their correlation with static and dynamic quenching efficiencies. *J. Phys. Chem.*, 100, 5541–5553.
5. Steenken, S. and Jovanovic, S. V. (1997) How easily oxidizable is DNA? One-electron reduction potentials of adenosine and guanosine radicals in aqueous solution. *J. Am. Chem. Soc.*, 119, 617–618.
6. Kasai, H. and Nishimura, S. (1984) Hydroxylation of deoxyguanosine at the C-8 position by ascorbic acid and other reducing agents. *Nucleic Acids Res.*, 12, 2137–2145.
7. Lindahl, T. (1993) Instability and decay of the primary structure of DNA. *Nature*, 362, 709–715.
8. Ohnishi, I., Iwashita, Y., Matsushita, Y., Ohtsuka, S., Yamashita, T., Inaba, K., Fukazawa, A., Ochiai, H., Matsumoto, K., Kurono, N., Matsushima, Y., Mori, H., Suzuki, S., Suzuki, S.,

Tanioka, F. and Sugimura, H. (2021) Mass spectrometric profiling of DNA adducts in the human stomach associated with damage from environmental factors. *Genes Environ.*, 43, 12.

9. Kamiya, H., Miura, K., Ishikawa, H., Inoue, H., Nishimura, S. and Ohtsuka, E. (1992) c-Ha-*ras* containing 8-hydroxyguanine at codon 12 induces point mutations at the modified and adjacent positions. *Cancer Res.*, 52, 3483–3485.
10. Moriya, M. (1993) Single-stranded shuttle phagemid for mutagenesis studies in mammalian cells: 8-oxoguanine in DNA induces targeted G•C→T•A transversions in simian kidney cells. *Proc. Natl. Acad. Sci. USA*, 90, 1122–1126.
11. Kamiya, H., Murata-Kamiya, N., Koizume, S., Inoue, H., Nishimura, S. and Ohtsuka, E. (1995) 8-Hydroxyguanine (7,8-dihydro-8-oxoguanine) in hot spots of the c-Ha-*ras* gene. Effects of sequence contexts on mutation spectra. *Carcinogenesis*, 16, 883–889.
12. Le Page, F., Margot, A., Grollman, A. P., Sarasin, A. and Gentil, A. (1995) Mutagenicity of a unique 8-oxoguanine in a human Ha-*ras* sequence in mammalian cells. *Carcinogenesis*, 16, 2779–2784.
13. Tan, X., Grollman, A. P. and Shibutani, S. (1999) Comparison of the mutagenic properties of 8-oxo-7,8-dihydro-2'-deoxyadenosine and 8-oxo-7,8-dihydro-2'-deoxyguanosine DNA lesions in mammalian cells. *Carcinogenesis*, 20, 2287–2292.
14. Satou, K., Kawai, K., Kasai, H., Harashima, H. and Kamiya, H. (2007) Mutagenic effects of 8-hydroxy-dGTP in live mammalian cells. *Free Radic. Biol. Med.*, 42, 1552–1560.

15. Satou, K., Hori, M., Kawai, K., Kasai, H., Harashima, H. and Kamiya, H. (2009) Involvement of specialized DNA polymerases in mutagenesis by 8-hydroxy-dGTP in human cells. *DNA Repair*, 8, 637–642.

16. Kamiya, H. (2003) Mutagenic potentials of damaged nucleic acids produced by reactive oxygen/nitrogen species: approaches using synthetic oligonucleotides and nucleotides. *Nucleic Acids Res.*, 31, 517–531.

17. Suzuki, T. and Kamiya H. (2017) Mutations induced by 8-hydroxyguanine (8-oxo-7,8-dihydroguanine), a representative oxidized base, in mammalian cells. *Genes Environ.*, 39, 2.

18. Kamiya, H., Yamazaki, D., Nakamura, E., Makino, T., Kobayashi, M., Matsuoka, I. and Harashima, H. (2015) Action-at-a-distance mutagenesis induced by oxidized guanine in Werner syndrome protein-reduced human cells. *Chem. Res. Toxicol.*, 28, 621–628.

19. Suzuki, T., Masuda, H., Mori, M., Ito, R. and Kamiya, H. (2021) Action-at-a-distance mutations at 5'-GpA-3' sites induced by oxidised guanine in WRN-knockdown cells. *Mutagenesis*, 36, 349–357.

20. Fukushima, R., Suzuki, T., Komatsu, Y. and Kamiya, H. (2022) Biased distribution of action-at-a-distance mutations by 8-oxo-7,8-dihydroguanine. *Mutation Res. (Fundam. Mol. Mech. Mutagen.)*, 825, 111794.

21. Suzuki, T., Zaima, Y., Fujikawa, Y., Fukushima, R. and Kamiya, H. (2022) Paradoxical role of the major DNA repair protein, OGG1, in action-at-a-distance mutation induction by 8-oxo-7,8-dihydroguanine. *DNA Repair (Amst)*, 111, 103276.

22. Pecori, R., Di Giorgio, S., Lorenzo, J. P. and Papavasiliou, F. N. (2022) Functions and consequences of AID/APOBEC-mediated DNA and RNA deamination. *Nat. Rev. Genet.*, 23, 505–518.

23. Alexandrov, L.B., Kim, J., Haradhvala, N.J. et al. (2020) The repertoire of mutational signatures in human cancer. *Nature*, 578, 94–101.

24. Lackey, L., Law, E. K., Brown, W. L. and Harris, R. S. (2013) Subcellular localization of the APOBEC3 proteins during mitosis and implications for genomic DNA deamination. *Cell Cycle*, 12, 762–772.

25. Constantin, D., Dubuis, G., Conde-Rubio, M. D. and Widmann, C. (2022) APOBEC3C, a nucleolar protein induced by genotoxins, is excluded from DNA damage sites. *FEBS J.*, 289, 808–831.

26. Suzuki, T., Harashima, H. and Kamiya, H. (2010) Effects of base excision repair proteins on mutagenesis by 8-oxo-7,8-dihydroguanine (8-hydroxyguanine) paired with cytosine and adenine. *DNA Repair*, 9, 542–550.

27. Kamiya, H., Yamaguchi, A., Suzuki, T. and Harashima, H. (2010) Roles of specialized DNA polymerases in mutagenesis by 8-hydroxyguanine in human cells. *Mutat. Res. (Fundam. Mol. Mech. Mutagen.)*, 686, 90–95.

28. Kamiya, H. and Kasai, H. (1997) Substitution and deletion mutations induced by 2-hydroxyadenine in *Escherichia coli*: effects of sequence contexts in leading and lagging strands. *Nucleic Acids Res.*, 25, 304–310.

29. Suzuki, T. and Kamiya, H. (2022) Easily-controllable, helper phage-free single-stranded phagemid production system. *Genes Environ.*, 44, 25.

30. Fukushima, R., Suzuki, T. and Kamiya, H. (2020) New indicator *Escherichia coli* strain for rapid and accurate detection of *supF* mutations. *Genes Environ*., 42, 28.

31. Schneider, C. A., Rasband, W. S. and Eliceiri, K. W. (2012) NIH Image to ImageJ: 25 years of image analysis. *Nat. Methods*, 9, 671–675.

32. Rouf Banday, A., Onabajo, O. O., Lin, S. H.-Y. et al. (2021) Targeting natural splicing plasticity of APOBEC3B restricts its expression and mutagenic activity. *Commun. Biol*., 4, 386.

33. Suzuki, T., Katayama, Y., Komatsu, Y. and Kamiya, H. (2019) Large deletions and untargeted substitutions induced by abasic site analog on leading versus lagging strand templates in human cells. *Mutagenesis*, 34, 421–429.

34. Parris, C. N. and Seidman, M. (1992) A signature element distinguishes sibling and independent mutations in a shuttle vector plasmid. *Gene*, 117, 1–5.

35. Chen, J., Miller, B. F. and Furano A. V. (2014) Repair of naturally occurring mismatches can induce mutations in flanking DNA. *eLife*, 3, e02001.

36. Adolph, M. B., Love, R. P., Feng, Y. and Chelico, L. (2017) Enzyme cycling contributes to efficient induction of genome mutagenesis by the cytidine deaminase APOBEC3B. *Nucleic Acids Res.*, 45, 11925–11940.

37. Burns, M. B., Lackey, L., Carpenter, M. A., Rathore, A., Land, A. M., Leonard, B., Refsland, E. W., Kotandeniya, D., Tretyakova, N., Nikas, J. B., Yee, D., Temiz, N. A., Donohue, D. E.,

McDougle, R. M., Brown, W. L., Law, E. K. and Harris, R. S. (2013) APOBEC3B is an enzymatic source of mutation in breast cancer. *Nature*, 494, 366–370.

38. Chan, K., Roberts, S. A., Klimczak, L. J., Sterling, J. F., Saini, N., Malc, E. P., Kim, J., Kwiatkowski, D. J., Fargo, D. C., Mieczkowski, P. A., Getz, G. and G. Gordenin, D. A. (2015) An APOBEC3A hypermutation signature is distinguishable from the signature of background mutagenesis by APOBEC3B in human cancers. *Nat. Genetics*, 47, 1067–1074.
39. Zuker, M. (2003) Mfold web server for nucleic acid folding and hybridization prediction. *Nucleic Acids Res.*, 31, 3406–3415.
40. Kawai, H., Iwata, R., Ebi, S., Sugihara, R., Masuda, S., Fujiwara, C., Kimura, S. and Kamiya, H. (2022) Development of a versatile high-throughput mutagenesis assay with multiplexed short read NGS using DNA-barcoded *supF* shuttle vector library amplified in *E. coli*. *eLife*, 11, e83780.
41. Buisson, R., Langenbucher, A., Bowen, D., Kwan, E. E., Benes, C. H., Zou, L. and Lawrence, M. S. (2019) Passenger hotspot mutations in cancer driven by APOBEC3A and mesoscale genomic features. *Science*, 364, eaaw2872.
42. Cortez, L. M., Brown, A. L., Dennis, M. A., Collins, C. D., Brown, A. J., Mitchell, D., Mertz, T. M. and Roberts, S. A. (2019) APOBEC3A is a prominent cytidine deaminase in breast cancer. *PLoS Genet.*, 15, e1008545.
43. Petljak, M., Dananberg, A., Chu, K., Bergstrom, E. N., Striepen, J., von Morgen, P., Chen, Y., Shah, H., Sale, J. E., Alexandrov, L. B., Stratton, M. R. and Maciejowski, J. (2022) Mechanisms of APOBEC3 mutagenesis in human cancer cells. *Nature*, 607, 799–807.

44. Yamazaki, H., Shirakawa, K., Matsumoto, T., Hirabayashi, S., Murakawa, Y., Kobayashi, M., Sarca, A. D., Kazuma, Y., Matsui, H., Maruyama, W., Fukuda, H., Shirakawa, R., Shindo, K., Ri, M., Iida, S. and Takaori-Kondo, A. (2019) Endogenous APOBEC3B overexpression constitutively generates DNA substitutions and deletions in myeloma cells. *Sci. Rep.*, 9, 7122.

45. Land, A. M., Law, E. K., Carpenter, M. A., Lackey, L., Brown, W. L. and Harris, R. S. (2013) Endogenous APOBEC3A DNA cytosine deaminase is cytoplasmic and nongenotoxic. *J. Biol. Chem.*, 288, 17253-17260.

Figure legends

Fig. 1 Knockdown of APOBEC3B by siRNA. (**A**) Amounts of APOBEC3B mRNA in U2OS cells upon si-APOBEC3B-A introduction. The amounts of mRNA were examined by RT-qPCR at 24, 48, and 72 h after siRNA treatment, and normalized relative to the amount of human GAPDH mRNA present in each sample. Values relative to those in U2OS cells treated with the control RNA (DS NC1 RNA) are shown. Experiments were performed in triplicate. The data obtained in a single experiment and the mean values are represented by circles and bars, respectively. (**B**) The levels of APOBEC3B expression in U2OS cells at 24, 48, and 72 h after siRNA introduction, detected by western blot analysis. Note that the 43K and 46K APOBEC3B isoforms are visualized [32]. C, cells treated with control DS NC1 RNA; KD, knockdown cells.

Fig. 2 Effects of the APOBEC3B knockdown on the *supF* mutant frequency induced by G^{O}. APOBEC3B was knocked down using si-APOBEC3B-A, and then the control G-plasmid and the modified G^{O}-plasmid were introduced into the knockdown cells. Transfection experiments were performed three times. Data are expressed as the means + standard errors. $^{**}P < 0.01$. control, cells treated with control DS NC1 RNA; si-A3B, cells treated with si-APOBEC3B-A.

Fig. 3 Effects of the APOBEC3B knockdown on the frequency of substitution mutations at 5'-GpA-3' dinucleotides (F_{GpA} value). APOBEC3B was knocked down using si-APOBEC3B-A.

Data are expressed as the means + standard errors. *$P < 0.05$. control, cells treated with control DS NC1 RNA; si-A3B, cells treated with si-APOBEC3B-A.

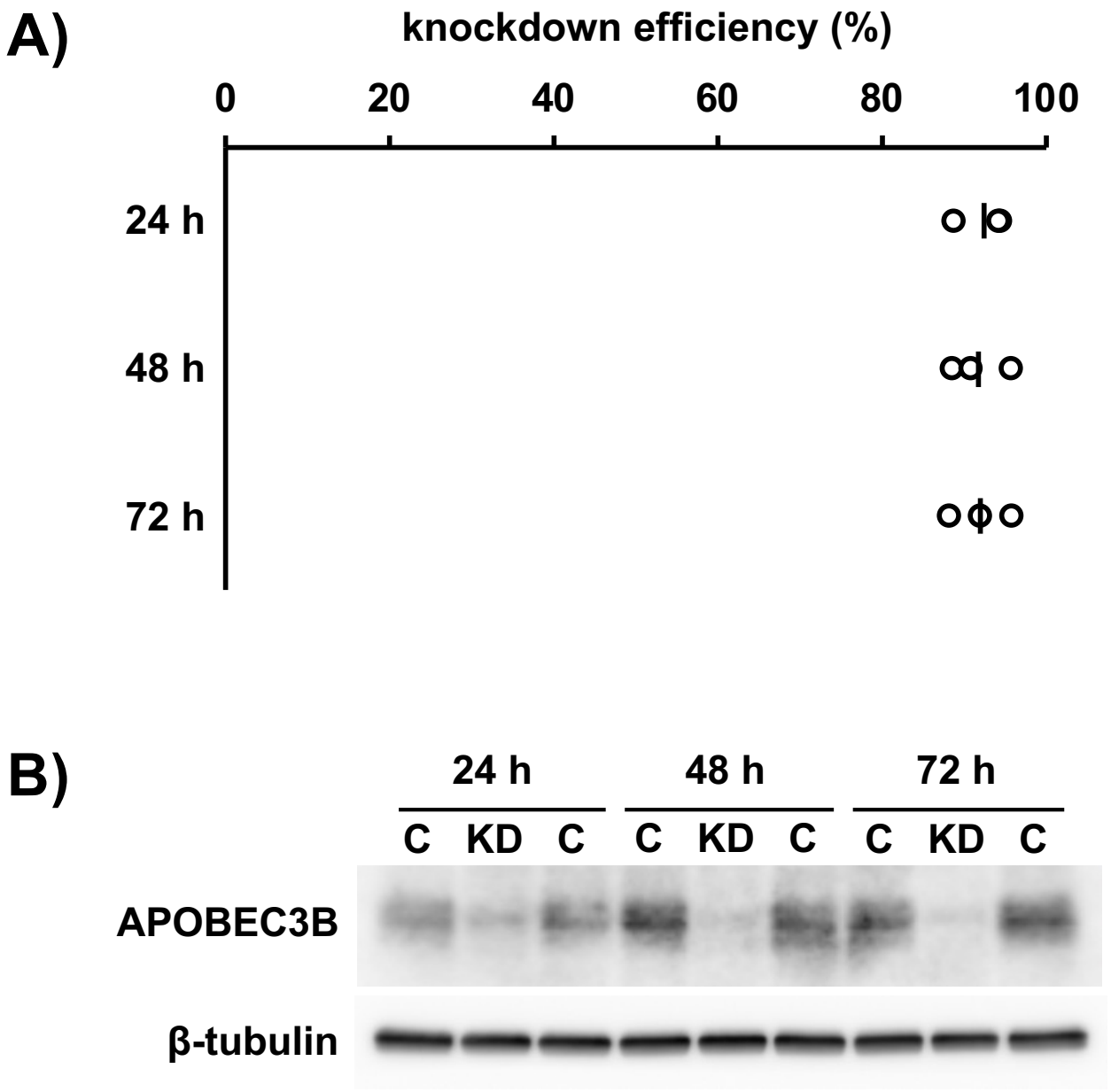
A)
knockdown efficiency (%)
0
20
40
60
80
100
24 h
48 h
72 h
B)
24 h
48 h
72 h
C
KD
C
C
KD
C
C
KD
C
APOBEC3B
β-tubulin

Fig. 1

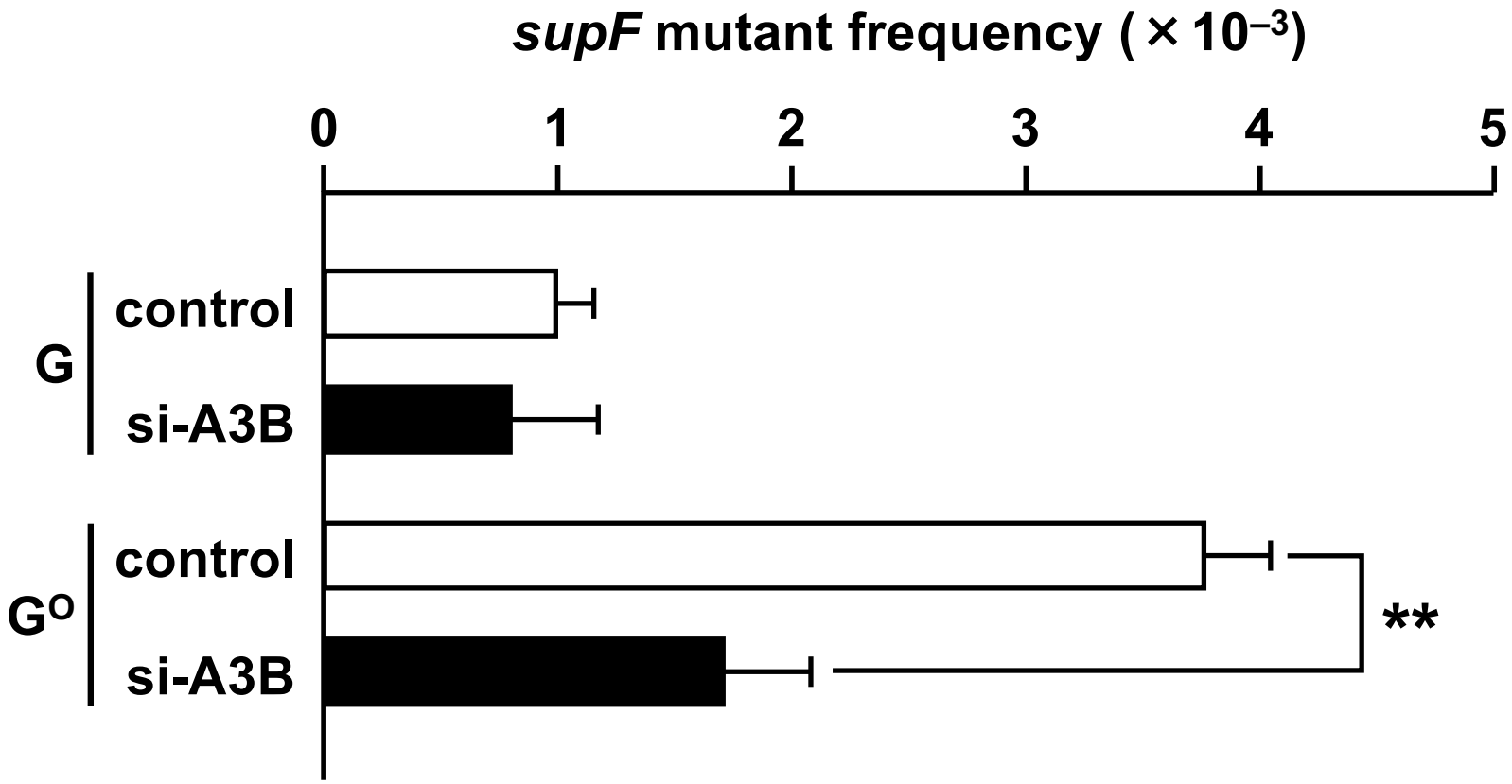
supF mutant frequency (× 10−3)
0
1
2
3
4
5
G
control
si-A3B
GO
control
si-A3B
**

Fig. 2

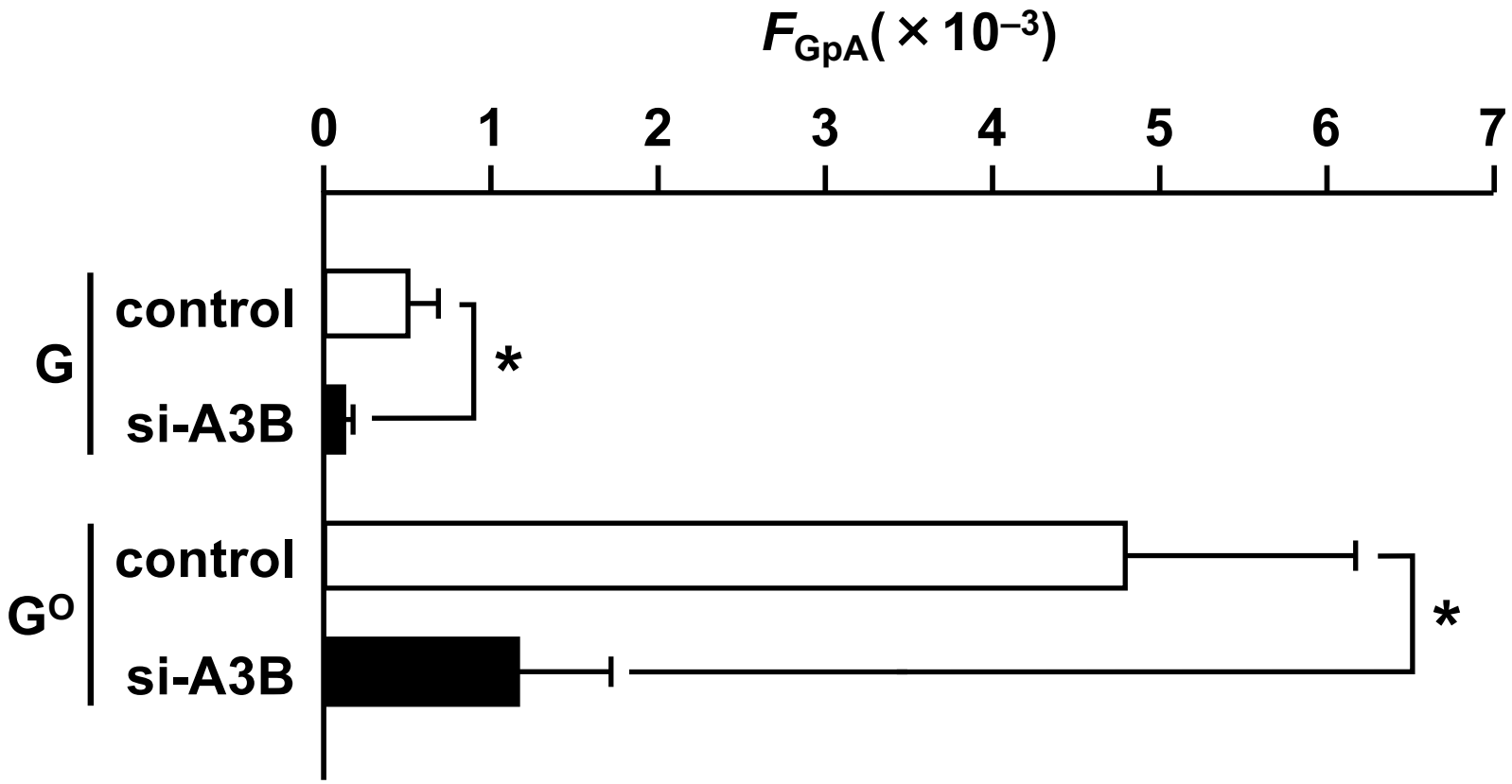

Fig. 3

Table 1 Overall mutation spectra[a]

	G		G^O	
	control	si-APOBEC3B-A	control	si-APOBEC3B-A
untargeted substitution				
at A:T pair	9 (13)	13 (19)	18 (26)	18 (26)
at G:C pair	66 (97)	72 (106)	110 (162)	78 (115)
targeted G:C → T:C	N.A.[b]	N.A.[b]	0 (0)	0 (0)
small insertion (1-2 bp)	0 (0)	0 (0)	0 (0)	0 (0)
large insertion (> 2 bp)	0 (0)	0 (0)	0 (0)	2 (3)
small deletion (1-2 bp)	3 (4)	0 (0)	0 (0)	0 (0)
large deletion (> 2 bp)	15 (22)	18 (26)	13 (19)	6 (9)
rearrangement or complex	11 (16)	9 (13)	10 (15)	10 (15)
unknown	4 (6)	2 (3)	1 (1)	1 (1)
total mutations	108	114	152	115
total colonies analyzed	68 (100)	68 (100)	68 (100)	68 (100)

[a]All data are represented as cases found (%).
[b]Not applicable.

Table 2 Untargeted base substitution mutations[a]

	G		G^O	
	control	si-APOBEC3B-A	control	si-APOBEC3B-A
transition				
A:T → G:C	4 (7)	4 (7)	2 (2)	2 (3)
G:C → A:T	19 (33)	17 (29)	32 (34)	16 (26)
transversion				
A:T → T:A	3 (5)	8 (14)	4 (4)	8 (13)
A:T → C:G	0 (0)	0 (0)	0 (0)	0 (0)
G:C → T:A	10 (17)	15 (26)	11 (12)	14 (23)
G:C → C:G	22 (38)	14 (24)	46 (48)	22 (35)
total base substitutions	58 (100)	58 (100)	95 (100)	62 (100)

[a]All data are represented as cases found (%). Barcode-identical colonies are excluded.

Table 3 Dinucleotide signatures of mutations at G and C[a]

	G		G^O	
	control	si-APOBEC3B-A	control	si-APOBEC3B-A
C mutations				
AC	0 (0)	1 (2)	0 (0)	1 (2)
TC	19 (37)	18 (39)	5 (6)	2 (4)
GC	0 (0)	3 (7)	1 (1)	3 (6)
CC	1 (2)	5 (11)	2 (2)	2 (4)
total C mutations	20 (39)	27 (59)	8 (9)	8 (15)
G mutations				
GA	25 (49)	8 (17)	71 (80)	31 (60)
GT	2 (4)	6 (13)	5 (6)	7 (13)
GG	4 (8)	4 (9)	5 (6)	4 (8)
GC	0 (0)	1 (2)	0 (0)	2 (4)
total G mutations	31 (61)	19 (41)	81 (91)	44 (85)
total base substitutions at G:C sites	51 (100)	46 (100)	89 (100)	52 (100)

[a]The sequence of the upper strand is shown. The percentages are shown in parentheses.